The Effect of Phosphate Treatment on Nickel Dispersion on MCM-41 Mesoporous Material

Sung Soo Park, Sang Joon Choe and Dong Ho Park[†]

Department of Chemistry, Inje University, Kyongnam, Kimhae 621-749, Korea

Abstract−The incorporation of nickel into mesoporous molecular sieves MCM-41 was carried out. Ni-PO/MCM41 and Ni-Cl/MCM41 were prepared by using Ni(II) acetate solution adjusted to pH=2.5 with phosphoric acid and hydrochloric acid, respectively, by the incipient wetness method. Photoacoustic spectroscopy (PAS) was used to study the local environments of Ni(II) incorporated into mesopores. The PAS of as-prepared Ni/MCM41, Ni-Cl/MCM41, and Ni-PO/MCM41 with Ni(II) acetate solution exhibits two bands of λ_{max} around 400 nm and 750 nm, which could be assigned to the $^3A_{2g} \rightarrow {}^3T_{1g}(F)$ and the $^3A_{2g} \rightarrow {}^3T_{1g}(P)$ transition of octahedral Ni(II) species. After calcination, Ni ion within Ni-PO/MCM41 dispersed atomically onto the surface of MCM-41 channel as an octahedral species without the transformation to nickel oxide phase, while Ni ion within Ni-Cl/MCM41 and Ni/MCM41 transformed to nickel oxide phase. It may be attributed to the fact that each Ni ion is separated by the phosphate grafted to surface silanol group. The effects of phosphoric acid on the dispersity of Ni ion within MCM-41 have been investigated using ^{31}P and ^{29}Si MAS NMR spectroscopy and X-ray photoelectron spectroscopy.

Key words: Incipient Wetness Method, MCM-41, Ni, Phosphate, Dispersion, Incorporation

INTRODUCTION

The mesoporous molecular sieve materials developed by Mobil in 1992 permit new possibilities for application as a catalyst for bulky molecules, as a support for various transition metal compounds, and as a host lattice for nanometer-sized materials. The pore diameter of MCM-41 with a hexagonal array of one-dimensional uniform mesopores can be tuned over 15-100 Å depending on the molecular length of surfactant template [Beck et al., 1992; Kresge et al., 1992]. Mesoporous molecular sieves containing redox active metals can be used as active catalysts for the oxidative transformation of bulky organic molecules. The incorporation of hetero-elements into a siliceous framework to modify the catalytic properties of the surface of mesoporous materials has been reported. Various metals such as B [Sayari et al., 1995], Al [Luan et al., 1995], Ga [Cheng et al., 1996], Ti [Corma et al., 1994; Tanev et al., 1994], V [Reddy et al., 1994], Cr [Ulagappan and Rao, 1996], Mn [Zhao and Goldfarb, 1995], Fe [Yuan et al., 1995], Co [Jentys et al., 1996], Sn [Das et al., 1995], and Zr [Kim et al., 1997] can be incorporated into the silica framework by the addition of metal sources. The high efficiency of hydrocracking of vacuum gasoline on NIMO-MCM-41 has been demonstrated [Corma et al., 1995].

In spite of the applicability as a catalyst for the bulky molecule of hetero-element containing mesoporous materials, the quality of mesoporous materials is, in general, deteriorated by the addition of hetero-elements, compared with purely siliceous mesoporous materials. A route to preparation of mesoporous metallosilicates via post-synthetic metal incorporation into frameworks of siliceous meso-porous materials has been suggested by Ryoo et al., in order to overcome deterioration in quality [Ryoo et al., 1997]. Park et al. also reported that Co in the presence of phosphate dispersed atomically onto the surface of MCM-41 using an incipient wetness method [Park et al., 1999]. This method coud be applied to the preparation of MCM-41 containing well dispersed Ni species. The preparation of MCM-41 containing atomically dispersed Ni species has not been reported.

The goal of this work is to incorporate an atomically dispersed Ni onto MCM-41 without a serious deterioration of silica framework and to investigate the effect of phosphoric acid on atomically dispersed incorporation of Ni(II) onto the surface of high quality MCM-41 using the incipient wetness method. The Ni-containing MCM-41 treated with phosphoric acid has been characterized by using photoacoustic spectroscopy (PAS) for the local environment of Ni and ^{31}P and ^{29}Si MAS solid-state NMR and X-ray photoelectron spectroscopy (XPS) for the effect of phosphoric acid on the dispersion of Ni.

EXPERIMENTAL

1. Preparation of MCM-41

The chemicals used in the synthesis were fumed silica (99.8%, metal free, Sigma), cetyltrimethylammonium bromide (CTABr) (99%, Fisons) and tetramethylammonium hydroxide (TMAOH) (25 wt% aqueous solution, Aldrich). Purely siliceous MCM-41 was synthesized following the literature procedure [Cheng et al., 1997]. TMAOH and CTABr were added to deionized water with stirring at 30 °C until the solution became clear. Then the fumed silica was added to the solution with stirring for 1 h. The molar composition of the final reaction gel, which is aged for 24 h at 20 °C, was 1.0 SiO_2 : 0.19 TMAOH : 0.27 CTABr : 40 H_2O. After aging, the mixture was reacted for 48 h at 150 °C in a Teflon-lined stainless steel

[†]To whom correspondence should be addressed.
E-mail: chempdh@ijnc.inje.ac.kr

autoclave. The product was filtered, washed with distilled water, dried in air at 60 °C and finally calcined at 550 °C for 8 h.

2. Characterization of MCM-41

XRD patterns were recorded with a Philips 1710 powder diffractometer with Cu K_α radiation (40 kV, 40 mA), 0.02° step size and 1 s step time. N_2 adsorption isotherms were measured at −196 °C with a gas sorption analyzer (Quantachrome Corp., Nova-2000). Before the experiments, samples were dehydrated at 350 °C for 12 h. The volume of adsorbed N_2 was normalized to the standard temperature and pressure. The calculation of the pore size distribution (PSD) was performed by using the Barrett-Joyner-Halenda (BJH) formula [Tanev and Vlaev, 1993]. The cumulative surface area of the mesopores was obtained from PSD curves.

3. Preparation of Ni-incorporated MCM-41

To prepare Ni-incorporated MCM-41, 0.1 g of MCM-41 was wetted and stirred for 5 h with 1 ml of nickel(II) acetate (99%, Fluka) solution of pH=2.5 controlled with phosphoric acid (85%, Junsei) or hydrochloric acid (35%, Osaka), and then dried at 80 °C for 5 h, afterward calcined at 700 °C for 3 h. The resultant sample treated with H_3PO_4 was designated Ni-PO/MCM41 and another one treated with HCl, Ni-Cl/MCM41.

4. Characterization of Ni-incorporated MCM-41

The method for UV-Vis spectrum of a powdered sample using a home-made photoacoustic spectrometer was described in detail in other literature [Lee and Chon, 1990]. According to Rosencwaig-Gersho theory for the photoacoustic effect, the acoustic signal in optically opaque and thermally thick solids is proportional to the optical absorption coefficient of the solid sample for the wavelength and varies as (the chopping frequency)$^{-3/2}$. PAS was recorded in the range of 350-800 nm and normalized by that of carbon black as a reference at the modulation frequency of 30 Hz.

^{31}P MAS NMR spectra were obtained on a Bruker DSX-400 (magnetic field 9.395 T, Lamor frequencies 161.98 MHz) spectrometer. Typical MAS speed of rotation was 10 KHz, and the delay time was 2.0 s. The 85% phosphoric acid was used as an external reference. ^{29}Si MAS NMR spectra were recorded at 7.05 T with a Varian Unity Plus 300 spectrometer with zirconia rotor in diameter 7.5 mm spun in air at 5 KHz. Spectra were acquired at 59.6 MHz with 90° pulses and 600 s recycle delays. Chemical shifts are given in ppm from the external tetramethylsilane.

X-ray photoelectron spectra were obtained by VG Microtech MT500 model electron spectrometer with X-ray excitation by using MgKα radiation.

RESULTS AND DISCUSSION

The quality of mesoporous molecular sieve MCM-41 was confirmed by XRD and N_2 sorption measurement. The XRD pattern of MCM-41 in Fig. 1 reflects a high quality of crystallites. The calcined MCM-41 has a d_{100} value of 44.4 Å, a pore diameter of 32.5 Å, and a surface area of 1,185 m^2/g.

Fig. 2 shows PAS for Ni/MCM41 treated with 0.04 M - nickel acetate by using the incipient wetness method. The PAS for dried Ni/MCM41 prior to calcination shows two bands of 398 nm and 747 nm, which could be assigned to $^3A_{2g} \rightarrow {}^3T_{1g}$(F) and $^3A_{2g} \rightarrow {}^3T_{1g}$(P) transitions of octahedral Ni(II) species [Anderson, 1972]. The $^3A_{2g} \rightarrow {}^3T_{2g}$ transition of octahedral Ni(II) species could not be occurring in
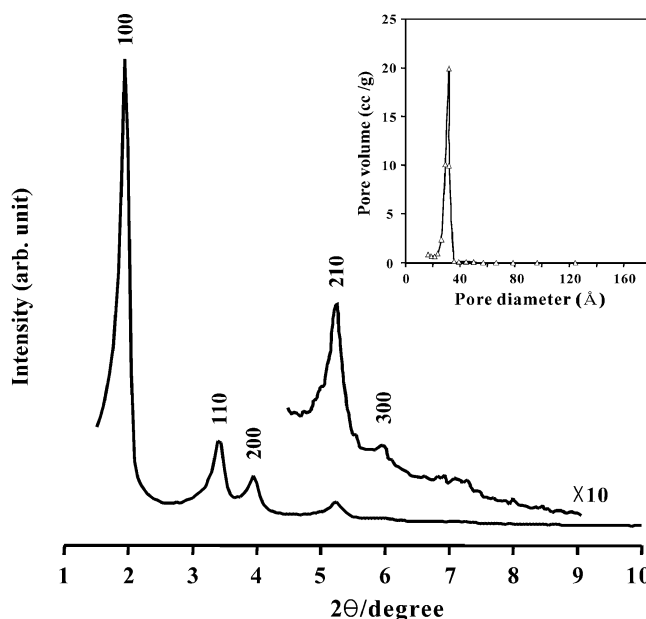

Fig. 1. X-ray diffraction patterns of calcined MCM-41. Inset shows pore size distribution curves for MCM-41 calculated from the desorption branch of the nitrogen adsorption isotherm using the BJH formula.
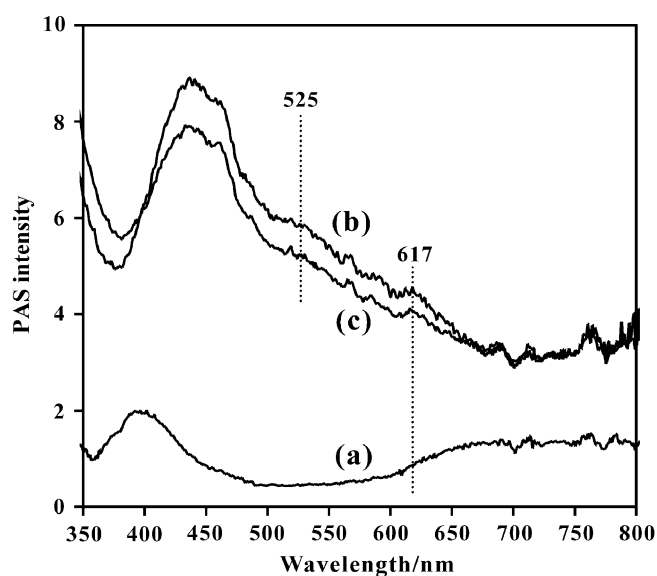

Fig. 2. PA spectra of Ni/MCM41 treated with 0.04 M - Ni(II) acetate solution and dried at 80 °C for 12 h (a), calcined sample (a) in air at 700 °C for 3 h (b) and dried sample (b) at 80 °C for 12 h after suspending with H_2O at room temperature for 1 h and recalcined in air at 700 °C for 3 h (c).

the visible range. Most of the surface of mesoporous molecular sieve MCM-41 is covered by silanol groups [Chen et al., 1995]. Ni(II) coordinated by silanol group or acetate ion or water has an octahedral structure. This result is similar to that for well-dispersed Ni(II) species on the surface of silica.

The Ni(II) species prior to calcination can be removed during washing. After calcination at 700 °C for 3 h, the intensity of PAS increased significantly, the maximum band red-shifted by 37 nm
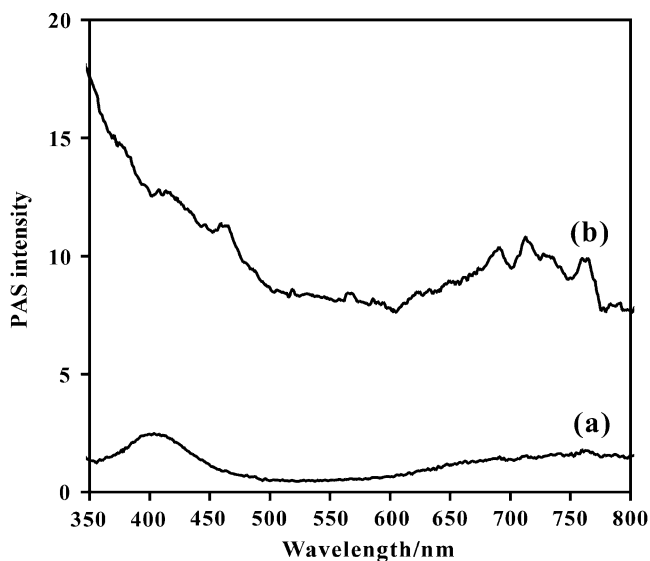
Fig. 3. PA spectra of Ni-Cl/MCM41 treated with 0.04 M - Ni(II) acetate solution at pH=2.5 controlled with HCl, and dried at 80 °C for 12 h (a) and calcined sample (a) in air at 700 °C for 3 h (b).

Fig. 4. PA spectra of Ni-PO/MCM41 treated with 0.04 M - Ni(II) acetate solution at pH=2.5 controlled with H₃PO₄, and dried at 80 °C for 12 h (a) and calcined sample (a) in air at 700 °C for 3 h(b).

and two shoulders at 525 nm and 617 nm appeared, comparing with that of dried Ni/MCM41. It may be attributable to the distorted octahedral Ni(II) species with low symmetry due to grafting onto the surface. The molar absorptivity for octahedral complexes of low symmetry is greater than that of symmetric octahedral complexes [Lever, 1986]. The surface silanol group coordinated to Ni(II) is deprotonated to be siloxy anion ($\equiv$Si-O$^-$) during calcination. The bond strength between Ni(II) and siloxy group is stronger than that between Ni(II) and silanol group due to the ionic character of bond. With PAS bands characteristic of the distorted octahedral Ni(II) species grafted on the surface of calcined Ni/MCM-41, the baseline of PAS in all ranges increased significantly. It indicates that part of Ni ions were transformed to the nickel oxide phase within the extraframework of MCM-41. The grafted Ni species and nickel oxide phase onto the surface remained intact during washing and recalcination, as shown in Fig. 2(c).

Fig. 3 shows PAS for Ni-Cl/MCM41 treated with 0.04 M - nickel acetate solution at pH=2.5 controlled with hydrochloric acid and dried 80 °C for 12 h. The PAS for dried Ni-Cl/MCM41 prior to calcination shows the bands of 403 nm and 761 nm, which could be assigned to $^3A_{2g} \rightarrow ^3T_{1g}$(F) and $^3A_{2g} \rightarrow ^3T_{1g}$(P) transitions of octahedral Ni(II) species [Anderson, 1972]. It is similar to PAS for dried Ni/MCM41 except of a slight shift to longer wavelength. After calcination in air at 700 °C for 3 h, the baseline of PAS increased significantly, indicative of the formation of extraframework nickel oxide cluster.

In order to obtain the highly dispersed Ni-containing MCM-41 without the formation of nickel oxide clusters, we have investigated the effect of phosphoric acid, which not only can react with the silanol groups on the surface of MCM-41, but also coordinate to nickel ion simultaneously. Fig. 4 shows PAS for Ni-PO/MCM41 treated with 0.04 M - nickel acetate solution at pH=2.5 controlled with phosphoric acid. PAS's for a dried sample [Fig. 4(a)] exhibit two bands of 404 nm and 754 nm corresponding to an octahedral Ni(II) [Ander-
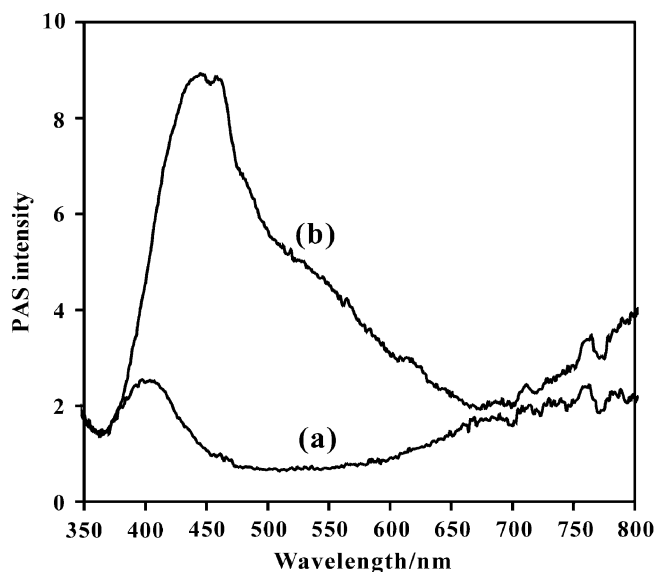
son, 1972]. It seems that Ni(II) is coordinated octahedrally by six ligating oxygen atoms in water molecules, silanol groups or phosphate ions. After calcination at 700 °C for 3 h, the intensity of PAS increased by about four times, the maximum band red-shifted by 34 nm and two shoulders in the range of 500 nm to 630 nm appeared, compared with that of dried Ni-PO/MCM41 [Fig. 4(b)]. This may be attributable to the distorted octahedral Ni(II) species with low symmetry [Lever, 1986]. There was no increase of baseline of PAS for Ni-PO/MCM41 during calcination, which is indicative of atomically well-dispersed nickel species in the absence of nickel oxide
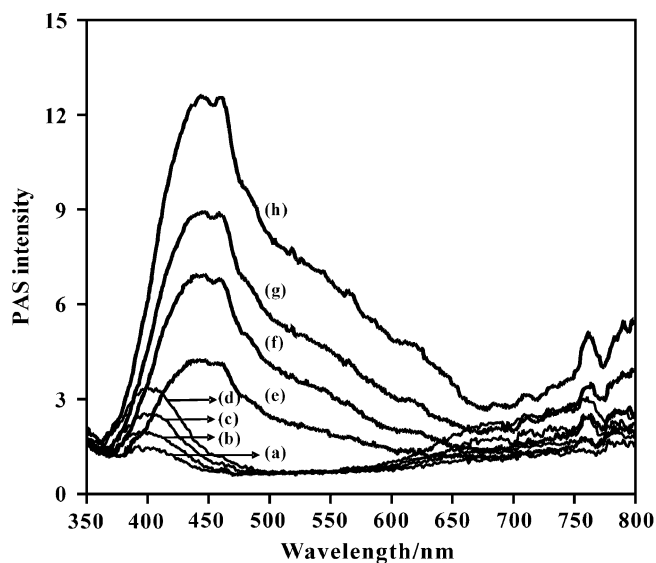

Fig. 5. PA spectra of Ni-PO/MCM41 treated with 0.01 M (a), 0.02 M (b), 0.04 M (c) and 0.08 M (d) - Ni(II) acetate solution at pH=2.5 controlled with H₃PO₄, dried at 80 °C for 12 h, and calcined Ni-PO/MCM41 [(e), (f), (g) and (h)) with sample (a), (b), (c) and (d), respectively].

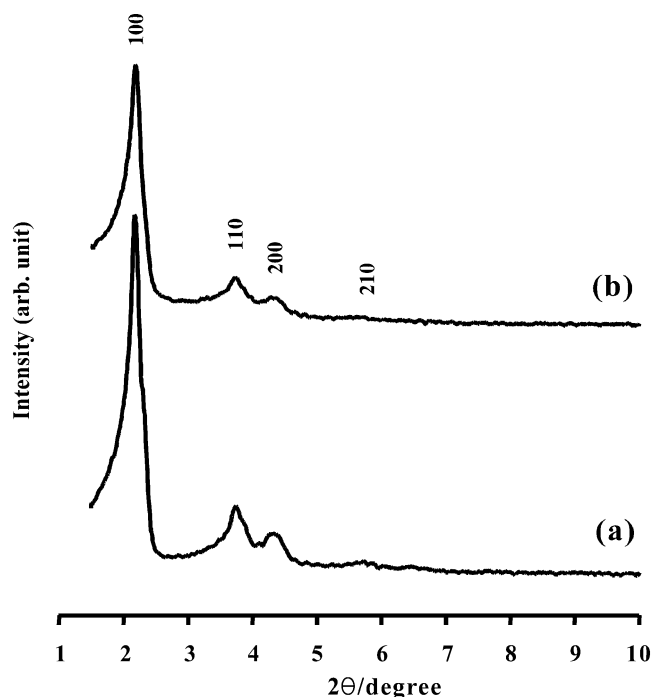Fig. 6. X-ray diffraction patterns of calcined MCM-41 after treatment with H_3PO_4 (a) and Ni-PO/MCM41 (b).

Fig. 7. ^{31}P MAS NMR spectra of dried MCM-41 at 80 °C for 12 h after treatment with H_3PO_4 solution (a), sample (a) calcined in air at 700 °C for 3 h (b), Ni-PO/MCM41 treated with 0.04 M - Ni(II) acetate solution at pH=2.5 controlled with H_3PO_4, dried at 80 °C for 12 h (c) and sample (c) calcined in air at 700 °C for 3 h (d).

cluster. The chloride ion disappeared and nickel ion transformed to nickel oxide during the calcination at 700 °C in air after treatment of hydrochloric acid. In case of phosphoric acid, the phosphate ion grafted on the surface played a role as a bridge between surface silanol groups and nickel ion.

Fig. 5 shows PAS for Ni-PO/MCM41 samples treated with 0.01 M, 0.02 M, 0.04 M, and 0.08 M - nickel acetate solution under the same conditions, respectively. The intensity of PAS for as-prepared and calcined samples at λ_{max} of 404 nm and 438 nm, respectively, increases with the content of Ni in MCM-41. The baseline for all PAS remains intact independent of Ni content. It can be taken as an evidence for atomically dispersed and octahedrally coordinated Ni ion under the effect of phosphate grafted to the surface of MCM-41.

Fig. 6 shows XRD patterns for calcined MCM-41 after treatment with phosphoric acid (a) and Ni-PO/MCM41 (b). Both XRD patterns illustrate typical peaks corresponding to diffraction at (100), (110), (200) and (210) plane of hexagonal phase. This reflects that the framework structure does not deteriorate seriously during treatment with phosphoric acid and Ni solution. The lowering of XRD intensity is caused by the decrease of surface regularity due to the grafted phosphate and coordinated Ni on the surface.

The ^{31}P MAS NMR spectra are displayed in Fig. 7. The dried sample at 80 °C for 12 h after being treated with the same amount of phosphoric acid as Ni-PO/MCM-41 exclusive of nickel acetate shows three peaks at 0.2, −10.8 and −23.1 ppm, as shown in Fig. 7(a). The peak at 0.2 ppm may be due to the pentavalent phosphorous of phosphoric acid molecules which are physically adsorbed at the MCM-41 surface [Bernstein et al., 1986]. The peak at −10.8 ppm indicates the presence of the isolated PO_4 group via the substitution of protons of surface silanol groups [Grimmer and Haubenreisser, 1983]. The peak at −23.1 ppm may be assigned to the presence of small amount of bridging PO_4 group [Bernstein et al., 1986].
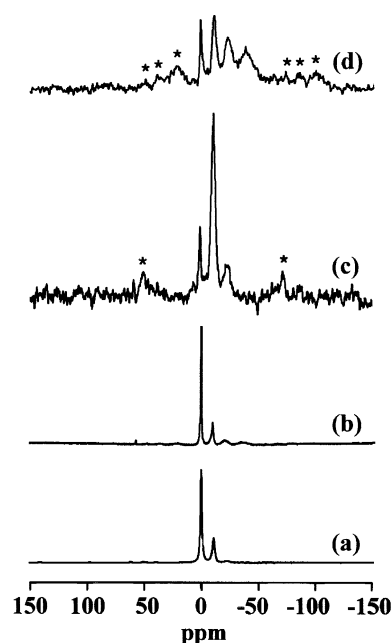
After calcination of this sample, the chemical shift value and width of peaks remained intact, which is indicative of the absence of polycrystalline phosphate cluster [Caro et al., 1990], as shown in Fig. 7(b). In the case of dried Ni-PO/MCM-41 compared with dried Ni-free PO/MCM-41, the intensity of both peaks at −10.7 and −21.3 ppm highly increases while that of 1.1 ppm decrease, all peaks are broadened and the chemical shift values are nearly unchanged, as shown in Fig. 7(c). Major part of phosphoric acid within Ni-free PO/MCM-41 is physically adsorbed at the MCM-41 surface as shown in Fig. 7(a), which indicates that most of phosphoric acid is not substituted to silanol group during drying. Therefore, the intensive peak at −10.7 ppm in the spectrum for dried Ni-PO/MCM-41 resulted not from the phosphate ion substituted to surface silanol group but from the phosphate ion that interacted with Ni ion coordinated by surface silanol group. Peak broadening also may be attributed to the interaction between phosphate and Ni ion. After calcination of Ni-PO/MCM-41, the peak at −22.6 ppm intensified and the peak at −38.3 ppm appeared. Phosphate group grafted to surface as well as silanol group can be coordinated to Ni ion. Ni atoms incorporated within MCM-41 could be dispersed highly without agglomerating to nickel oxide phase due to the influence of phosphoric acid. From the result that P/Ni ratio measured by EDX was 2.8. Ni ion is, possibly, surrounded by two or three phosphate.

The ^{29}Si MAS NMR spectra for tetrahedral silicon in MCM-41 consist of three lines at −91, −101, and −110 ppm resulting from $Si(OSi)_2(OH)_2$ (Q^2), $Si(OSi)_3(OH)$ (Q^3), and $Si(OSi)_4$ (Q^4) structural units, respectively [Maciel et al., 1994]. The Q^2 and Q^3 silicon ratio of dried Ni-PO/MCM41 [Fig. 8(b)] is higher than that of calcined MCM-41 [Fig. 8(a)]. The fraction of Q^2, Q^3, and Q^4 obtained from fitted curves for dried Ni-PO/MCM41 is 14.9, 67.7, and 17.4%,
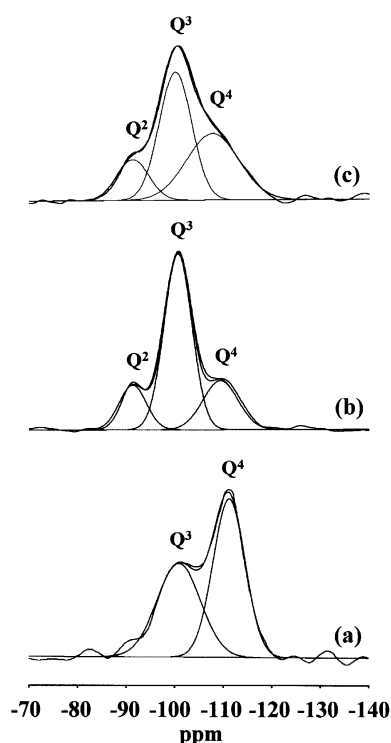
Fig. 8. ^{29}Si MAS NMR spectra of calcined MCM-41 (a), dried Ni-PO/MCM41 at 80 °C for 12 h after treatment with 0.04 M - Ni(II) acetate solution at pH=2.5 controlled with H₃PO₄ (b) and sample (b) calcined in air at 700 °C for 3 h (c).

Table 1. Binding energy (eV) values of Ni 2p$_{3/2}$ and P 2p and atomic ratios of Si/Ni and P/Ni for Ni-PO/MCM41 calcined at 700 °C for 3 h after being treated with Ni(II) acetate solution with various concentration at pH=2.5 controlled with H₃PO₄

Concentration of impregnated Ni(II) solution (M)	B.E. (eV)			E$_{Sat.}^{b}$ (eV)	Si/Ni^c	P/Ni^c
	Ni 2p$_{3/2}$	Sat.^{a}	P 2p			
0.02	856.6	861.0	133.7	4.4	183.5	3.4
0.04	858.1	862.6	134.1	4.5	121.6	3.3
0.08	857.1	862.2	134.0	5.1	52.6	3.6

^{a}Binding energy of the satellite for Ni 2p$_{3/2}$.
^{b}Energy separation between the Ni 2p$_{3/2}$ and the satellite for Ni 2p$_{3/2}$.
^{c}Atomic ratio as determined by XPS analysis.

may be attributed to the fact that the condensation of silanol group is prohibited by the phosphate grafted on the surface of Ni-PO/MCM41. The grafted phosphate on the surface of MCM-41 with plenty of Q^3 units makes it possible to stabilize the dispersed Ni(II).

Fig. 9 shows photoelectron spectroscopies for Ni 2p$_{3/2}$ (A) and P 2p (B) region of Ni-PO/MCM41 samples. These samples treated with 0.02 M (a), 0.04 M (b) and 0.08 M (c) - Ni(II) acetate solution controlled at pH=2.5 with phosphoric acid, dried at 80 °C for 12 h and calcined at 700 °C for 3 h. The intensities of Ni and P peaks increased with increasing the concentration of Ni acetate solution. In order to maintain the pH of 2.5, the amount of phosphoric acid in the solution increases with increasing the concentration of Ni acetate solution. Table 1 illustrates the binding energies of Ni 2p$_{3/2}$, its satellite peak and P 2p, and the molar ratios of Si/Ni and P/Ni. The ratio of P to Ni measured by XPS were 3.4 (a), 3.3 (b), and 3.6 (c), respectively, whose values are nearly the same. The ratio of Si to Ni decreases with increase of the concentration of Ni(II) solution, as expected. The difference of binding energy between Ni 2p$_{3/2}$ and its satellite peak, which is designated by BE in Table 1, reflects the chemical environment of Ni(II) in Ni-PO/MCM41. BE's of Ni-PO/MCM41 treated with remaining nearly intact P/Ni ratio are nearly the same as shown in Table 1, which is attributable to the formation of Ni ion surrounded by two or three phosphates on the surface of silicious MCM-41 without nickel oxide phase [Khawaja et al., 1995]. The BE of Ni 2p$_{3/2}$ for Ni/MCM-41 treated with 0.04 M - Ni acetate solution free from phosphoric acid was 5.8 eV (not shown), which is indicative of the formation of nickle oxide phase. The binding energies of ca. 134 eV of P 2p in Fig. 9(B) are nearly the same as that of nickel phosphate, which is indicative of the direct interaction between PO₄ tetrahedra and Ni(II). This value is compared with that of P₂O₅ phase, which has a higher value of 134.7 eV.

The metal dispersion onto a support affects the effectiveness of the catalytic element. In this study, we could prepare the mesoporous material MCM-41 including the highly dispersed Ni by treatment with phosphoric acid.

respectively. This indicates that part of surface siloxanes is hydrolyzed to silanol group by phosphoric acid. The fraction of Q^2, Q^3, and Q^4 for calcined Ni-PO/MCM41 is 12.7, 56.4, and 31.0%, respectively [Fig. 8(c)]. Although the fraction of Q^4 unit increases with calcination, it is much lower than that of calcined MCM-41 (44.5% and 55.5% for Q^3 and Q^4, respectively), as shown in Fig. 8(a). This
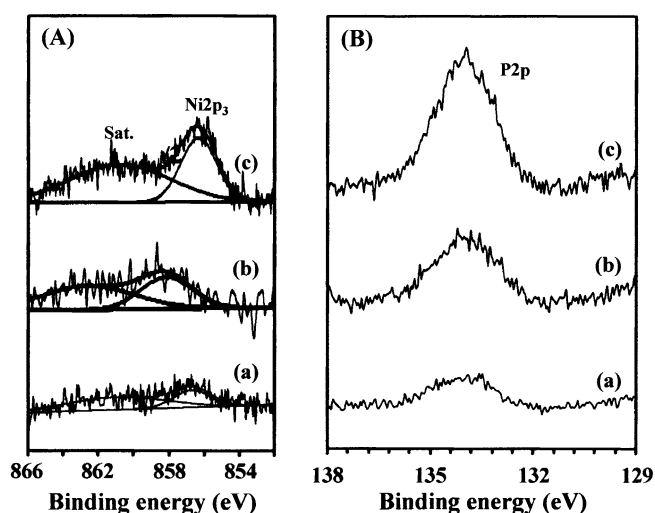

Fig. 9. XPS of the Ni 2p$_{3/2}$ (A) and the P 2p (B) for Ni-PO/MCM41 dried at 80 °C for 12 h and calcined at 700 °C for 3 h after treated with 0.02 M (a), 0.04 M (b) and 0.08 M (c) - Ni(II) acetate solution at pH=2.5 controlled with H₃PO₄, respectively.

CONCLUSION

Ni ion within Ni-PO/MCM41 dispersed atomically onto the sur-

face of MCM-41 channel as an octahedral species without the transformation to Ni oxide phase, while Ni ion within Ni-Cl/MCM41 and Ni/MCM41 was transformed to Ni oxide phase. The remaining of PAS baseline intensity for Ni-PO/MCM41 during calcination is indicative of atomically well-dispersed nickel species in the absence of nickel oxide cluster. The framework structure does not deteriorate seriously during treatment with Ni(II) acetate solution containing phosphoric acid. Ni ion coordinated by phosphate group grafted to siliceous surface dispersed highly without agglomerating to nickel oxide phase due to the influence of phosphoric acid.

REFERENCES

Anderson, J. H., "A Study of Water and Ammonia Adsorption on Silica Supported Ni(II) Using Visible and Near Infrared Spectroscopy," *J. Catal.*, **26**, 277 (1972).

Beck, J. S., Vartuli, J. C., Roth, W. J., Leonowicz, M. E., Kresge, C. T., Schmitt, K. D., Chu, C. T.-W., Olsen, D. H., Sheppard, E. W., McCullen, S. B., Higgins, J. B. and Schlenker, J. L., "A New Family of Mesoporous Molecular Sieves Prepared with Liquid Crystal Templates," *J. Am. Chem. Soc.*, **144**, 10834 (1992).

Bernstein, T., Fink, P., Mastikhin, V. M. and Shubin, A. A., "High-resolution Solid-state Magic Angle Spinning Magnetic Resonance Investigations of Surface Hydroxy Groups on Modified Silica Gel," *J. Chem. Soc., Faraday Trans. 1*, **82**, 1879 (1986).

Caro, J., Bolow, M., Derewinski, M., Haber, J., Hunger, M., Karger, J., Pfeifer, H., Storek. W. and Zibrowius, B., "NMR and IR Studies of Zeolite H-ZSM-5 Modified with Orthophosphoric Acid," *J. Catal.*, **124**, 367 (1990).

Cheng, C.-F., He, H., Zhou, W., Klinowski, J., Sousa Goncalves, J. A. and Gladden, L. F., "Synthesis and Characterization of the Gallosilicate Mesoporous Molecular Sieve MCM-41," *J. Phys. Chem.*, **100**, 390 (1996).

Cheng, C.-F., Park, D. H. and Klinowski, J., "Optimal Parameter for the Synthesis of the Mesoporous Molecular Sieve [Si]-MCM-41," *J. Chem. Soc.*, *Faraday Trans.*, **93**(1), 193 (1997).

Chen, J., Li, Q., Xu, R. and Xiao, F., "Distinguishing the Silanol Groups in the Mesoporous Molecular Sieve MCM-41," *Angew. Chem. Int. Ed. Engl.*, **34**, 2694 (1995).

Corma, A., Martinez-Sora, M. V. and Monton, J. B., "Hydrocracking of Vacuum Gasoil on the Novel Mesoporous MCM-41 Aluminosilicate Catalyst," *J. Catal.*, **153**, 25 (1995).

Corma, A., Navarro, M. T. and Pérez-Pariente, J., "Synthesis of an Ultralarge Pore Titanium Silicate Isomorphous to MCM-41 and its Application as a Catalyst for Selective Oxidation of Hydrocarbons," *J. Chem. Soc. Chem. Commun.*, 147 (1994).

Das, T. Kr., Chaudhari, K., Chandwadkar, A. J. and Sivasanker, S., "Synthesis and Catalytic Properties of Mesoporous Tin Silicate Molecular Sieves," *J. Chem. Soc., Chem. Commun.*, 2495 (1995).

Grimmer, A.-R. and Haubenreisser, U., "High-field Static and MAS ^{31}P NMR: Chemical Shift Tensors of Polycrystalline Potassium Phosphates $P_2O_5 \cdot xK_2O(0 \leq x \leq 3)$," *Chem. Phys. Letters*, **99**, 487 (1983).

Jentys, A., Pham, N. H., Vinek, H., English, M. and Lercher, J. A., "Synthesis and Characterization of Mesoporic Materials Containing Highly Dispersed Cobalt," *Microporous Mater.*, **6**, 13 (1996).

Kim, A., Bruinsman, P., Chen, Y., Wang, L.-Q. and Liu, J., "Amphoteric Surfactant Templating Route for Mesoporous Zirconia," *Chem. Commun.*, 161 (1997).

Khawaja, E. E., Durrani, S. M. A., Al-Adel, F. F., Salim, M. A. and Sakhawat Hussain, M., "X-ray Photoelectron Spectroscopy and Fourier Transform-infrared Studies of Transition Metal Phosphate Glasses," *J. Mater. Sci.*, **30**, 225 (1995).

Kresge, C. T., Leonowicz, M. E., Roth, W. J., Vartuli, J. C. and Beck, J. S., "Ordered Mesoporous Molecular Sieves Synthesized by a Liquid-crystal Template Mechanism," *Nature*, **359**, 710 (1992).

Lee, K. Y. and Chon, H., "Photoacoustic Spectroscopy Study of CoAPO-5 and CoZSM-5 Molecular Sieves," *J. Catal.*, **126**, 677 (1990).

Lever, A. B. P. In "Inorganic Electronic Spectroscopy," Elsevier, New York, chapter 4 (1986).

Luan, Z., Cheng, C.-F., Zhou, W. and Klinowski, J., "Mesopore Molecular Sieve MCM-41 Containing Framework Aluminum," *J. Phys. Chem.*, **99**, 1018 (1995).

Maciel, G. E. and Ellis, P. D. In "NMR Techniques in Catalysis," Eds. Bell, A. T., Pines, A. (Eds.), Marcel Dekker, New York, 234 (1994).

Park, D. H., Park, S. S. and Choe, S. J., "Photoacoustic Spectroscopic Study on Cobalt Incorporation onto the Surface of Mesoporous Molecular Sieves," *Bull. Korean Chem. Soc.*, **20**, 715 (1999).

Reddy, K. M., Moudrakovski, I. and Sayari, A., "Synthesis of Mesoporous Vanadium Silicate Molecular Sieves," *J. Chem. Soc. Chem. Commun.*, 1059 (1994).

Ryoo, R., Jun, S., Kim, J. M. and Kim, M. J., "Generalised Route to the Preparation of Mesoporous Metallosilicates via Post-synthetic Metal Implantation," *Chem. Commun.*, 2225 (1997).

Sayari, A., Danuman, C. and Moudrakovski, I. L., "Boron-Modified MCM-41 Mesoporous Molecular Sieves," *Chem. Mater.*, **7**, 813 (1995).

Tanev, P. T., Chibwe, M. and Pinnavaia, T. J., "Titanium-containing Mesoporous Molecular Sieves for Catalytic Oxidation of Aromatic Compounds," *Nature* (*London*), **368**, 321 (1994).

Tanev, P. T. and Vlaev, L. T., "An Attempt at a More Precise Evaluation of the Approach to Mesopore Size Distribution Calculations Depending on the Degree of Pore Blocking," *J. Colloid Interface Sci.*, **160**, 110 (1993).

Ulagappan, N. and Rao, C. N. R., "Synthesis and Characterization of the Mesoporous Chromium Silicates Cr-MCM-41," *Chem. Commun.*, 1047 (1996).

Yuan, Z. Y., Liu, S. Q., Chen, T. H., Wang, J. Z. and Li, H. X., "Synthesis of Iron-containing MCM-41," *J. Chem. Soc., Chem. Commun.*, 973 (1995).

Zhao, D. Y. and Goldfarb, D., "Synthesis of Mesoporous Manganosilicates: Mn-MCM-41, Mn-MCM-48 and Mn-MCM-L," *J. Chem. Soc. Chem. Commun.*, 875 (1995).